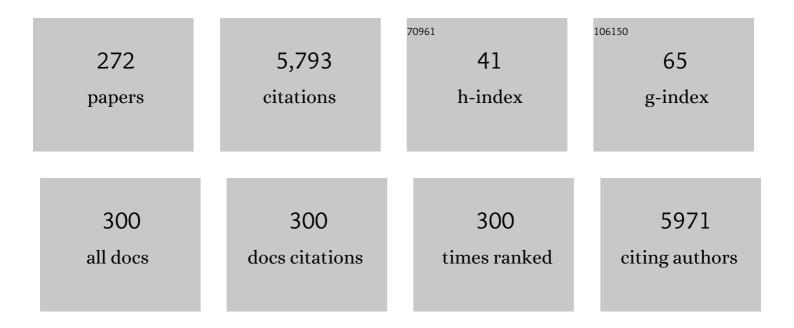
List of Publications by Year in descending order

Source: https://exaly.com/author-pdf/9134046/publications.pdf Version: 2024-02-01



<u> Redt ΜΑΊμιες</u>

#	Article	IF	CITATIONS
1	Shear-stress sensitive lenticular vesicles for targeted drug delivery. Nature Nanotechnology, 2012, 7, 536-543.	15.6	248
2	The morphology of anisotropic 3D-printed hydroxyapatite scaffolds. Biomaterials, 2008, 29, 3799-3806.	5.7	190
3	Circulating levels of copeptin, a novel biomarker, in lower respiratory tract infections. European Journal of Clinical Investigation, 2007, 37, 145-152.	1.7	179
4	Strained-layer growth and islanding of germanium on Si(111)-(7 × 7) studied with STM. Surface Science, 1991, 248, 321-331.	0.8	177
5	Microstructure of selective laser melted nickel–titanium. Materials Characterization, 2014, 94, 189-202.	1.9	176
6	Tailoring Selective Laser Melting Process Parameters for NiTi Implants. Journal of Materials Engineering and Performance, 2012, 21, 2519-2524.	1.2	171
7	Impaired Action of Thyroid Hormone Associated with Smoking in Women with Hypothyroidism. New England Journal of Medicine, 1995, 333, 964-969.	13.9	149
8	High-resolution tomographic imaging of a human cerebellum: comparison of absorption and grating-based phase contrast. Journal of the Royal Society Interface, 2010, 7, 1665-1676.	1.5	149
9	Haemostatic profile in hypothyroidism as potential risk factor for vascular or thrombotic disease. European Journal of Clinical Investigation, 2001, 31, 131-137.	1.7	119
10	Layer-by-layer growth of germanium on Si(100): strain-induced morphology and the influence of surfactants. Ultramicroscopy, 1992, 42-44, 832-837.	0.8	111
11	Biomimetic Remineralization of Carious Lesions by Self-Assembling Peptide. Journal of Dental Research, 2017, 96, 790-797.	2.5	103
12	Comparison of Microfocus- and Synchrotron X-ray Tomography for the Analysis of Osteointegration around Ti6Al4V Implants. , 2004, 7, 42-51.		101
13	Impact of nanometer-scale roughness on contact-angle hysteresis and globulin adsorption. Journal of Vacuum Science & Technology an Official Journal of the American Vacuum Society B, Microelectronics Processing and Phenomena, 2001, 19, 1715.	1.6	90
14	Initial stages of Cu epitaxy on Ni(100): Postnucleation and a well-defined transition in critical island size. Physical Review B, 1996, 54, 17858-17865.	1.1	84
15	Protein adsorption and monocyte activation on germanium nanopyramids. Biomaterials, 2001, 22, 2307-2316.	5.7	80
16	Highâ€resolution Xâ€ray tomography of the human inner ear: synchrotron radiationâ€based study of nerve fibre bundles, membranes and ganglion cells. Journal of Microscopy, 2009, 234, 95-102.	0.8	78
17	Differentiation of human mesenchymal stem cells on plasma-treated polyetheretherketone. Journal of Materials Science: Materials in Medicine, 2014, 25, 515-525.	1.7	77
18	Dimer Pairing on the C-Alloyed Si(001) Surface. Physical Review Letters, 1999, 82, 972-975.	2.9	73

#	Article	IF	CITATIONS
19	Non-destructive three-dimensional evaluation of a polymer sponge by micro-tomography using synchrotron radiation. New Biotechnology, 2002, 19, 73-78.	2.7	73
20	The use of shear stress for targeted drug delivery. Cardiovascular Research, 2013, 99, 328-333.	1.8	72
21	Position paper from the IBRA Symposium on Surgery of the Head – The 2nd International Symposium for Condylar Fracture Osteosynthesis, Marseille, France 2012. Journal of Cranio-Maxillo-Facial Surgery, 2014, 42, 1234-1249.	0.7	70
22	Extending two-dimensional histology into the third dimension through conventional micro computed tomography. NeuroImage, 2016, 139, 26-36.	2.1	69
23	Nanostructure of healthy and caries-affected human teeth. Nanomedicine: Nanotechnology, Biology, and Medicine, 2011, 7, 694-701.	1.7	68
24	Resorbable defect analog PLGA scaffolds using CO2as solvent: Structural characterization. Journal of Biomedical Materials Research Part B, 2002, 62, 89-98.	3.0	65
25	An optimization procedure for spatial and density resolution in hard X-ray micro-computed tomography. Nuclear Instruments & Methods in Physics Research B, 2004, 225, 599-603.	0.6	62
26	Three-dimensional strain fields in human brain resulting from formalin fixation. Journal of Neuroscience Methods, 2011, 202, 17-27.	1.3	62
27	Strain Relief at Metal Interfaces with Square Symmetry. Physical Review Letters, 1996, 76, 2358-2361.	2.9	58
28	Circulating levels of pro-atrial natriuretic peptide in lower respiratory tract infections. Journal of Internal Medicine, 2006, 260, 568-576.	2.7	58
29	Multimodal imaging of human cerebellum - merging X-ray phase microtomography, magnetic resonance microscopy and histology. Scientific Reports, 2012, 2, 826.	1.6	57
30	Tomographic brain imaging with nucleolar detail and automatic cell counting. Scientific Reports, 2016, 6, 32156.	1.6	57
31	Complementary X-ray tomography techniques for histology-validated 3D imaging of soft and hard tissues using plaque-containing blood vessels as examples. Nature Protocols, 2014, 9, 1401-1415.	5.5	55
32	High density resolution in synchrotron-radiation-based attenuation-contrast microtomography. Proceedings of SPIE, 2008, , .	0.8	53
33	Island Shape Transition in Heteroepitaxial Metal Growth on Square Lattices. Physical Review Letters, 1998, 80, 2642-2645.	2.9	50
34	Artificial Muscle Devices: Innovations and Prospects for Fecal Incontinence Treatment. Annals of Biomedical Engineering, 2016, 44, 1355-1369.	1.3	47
35	Comparison between x-ray tube-based and synchrotron radiation-based μCT. Proceedings of SPIE, 2008, , .	0.8	46
36	Three-dimensional quantification of capillary networks in healthy and cancerous tissues of two mice. Microvascular Research, 2012, 84, 314-322.	1.1	46

#	Article	IF	CITATIONS
37	Experimental comparison of grating- and propagation-based hard X-ray phase tomography of soft tissue. Journal of Applied Physics, 2014, 116, .	1.1	46
38	Bony labyrinth morphology clarifies the origin and evolution of deer. Scientific Reports, 2017, 7, 13176.	1.6	45
39	Hard Xâ€Ray Nanoholotomography: Largeâ€Scale, Labelâ€Free, 3D Neuroimaging beyond Optical Limit. Advanced Science, 2018, 5, 1700694.	5.6	45
40	Self-Assembly in Ultrahigh Vacuum:Â Growth of Organic Thin Films with a StableIn-PlaneDirectional Order. Journal of the American Chemical Society, 1998, 120, 8563-8564.	6.6	44
41	Morphology of bony tissues and implants uncovered by high-resolution tomographic imaging. International Journal of Materials Research, 2007, 98, 613-621.	0.1	44
42	MBE growth of para-hexaphenyl on GaAs(001)-2×4. Surface Science, 1998, 418, 256-266.	0.8	43
43	In situ scanning tunneling microscopy study of C-induced Ge quantum dot formation on Si(100). Applied Physics Letters, 1999, 74, 994-996.	1.5	42
44	High-resolution tomographic imaging of microvessels. Proceedings of SPIE, 2008, , .	0.8	42
45	Combined use of micro computed tomography and histology to evaluate the regenerative capacity of bone grafting materials. International Journal of Materials Research, 2014, 105, 679-691.	0.1	42
46	Reduction of the bacterial load by the silver-coated endotracheal tube (SCET), a laboratory investigation. Technology and Health Care, 1999, 7, 359-370.	0.5	38
47	Siloxane-based thin films for biomimetic low-voltage dielectric actuators. Sensors and Actuators A: Physical, 2015, 233, 32-41.	2.0	38
48	Electrospraying Nanometerâ€Thin Elastomer Films for Lowâ€Voltage Dielectric Actuators. Advanced Electronic Materials, 2016, 2, 1500476.	2.6	37
49	Holotomography versus X-ray grating interferometry: A comparative study. Applied Physics Letters, 2013, 103, .	1.5	36
50	Oblique Incidence Organic Molecular Beam Deposition and Nonlinear Optical Properties of Organic Thin Films with a Stable In-Plane Directional Order. Advanced Materials, 1999, 11, 745-749.	11.1	34
51	Surface patterned polymer micro-cantilever arrays for sensing. Sensors and Actuators A: Physical, 2011, 172, 2-8.	2.0	33
52	Rapid prototyped porous nickel–titanium scaffolds as bone substitutes. Journal of Tissue Engineering, 2014, 5, 204173141454067.	2.3	33
53	Prenatal growth stages show the development of the ruminant bony labyrinth and petrosal bone. Journal of Anatomy, 2017, 230, 347-353.	0.9	33
54	Recent developments in x-ray Talbot interferometry at ESRF-ID19. Proceedings of SPIE, 2010, , .	0.8	32

#	Article	IF	CITATIONS
55	Three-dimensional registration of tomography data for quantification in biomaterials science. International Journal of Materials Research, 2012, 103, 242-249.	0.1	32
56	NATURAL FORMATION OF NANOSTRUCTURES: FROM FUNDAMENTALS IN METAL HETEROEPITAXY TO APPLICATIONS IN OPTICS AND BIOMATERIALS SCIENCE. Surface Review and Letters, 2001, 08, 169-228.	0.5	31
57	Nondestructive three-dimensional evaluation of biocompatible materials by microtomography using synchrotron radiation. , 2002, , .		31
58	Automatic selection of a representative trial from multiple measurements using Principle Component Analysis. Journal of Biomechanics, 2012, 45, 2306-2309.	0.9	30
59	Understanding Nano-Anatomy of Healthy and Carious Human Teeth: a Prerequisite for Nanodentistry. Biointerphases, 2012, 7, 4.	0.6	30
60	Nanostructure of carious tooth enamel lesion. Acta Biomaterialia, 2014, 10, 355-364.	4.1	30
61	The bony labyrinth of toothed whales reflects both phylogeny and habitat preferences. Scientific Reports, 2018, 8, 7841.	1.6	29
62	Strain fields in histological slices of brain tissue determined by synchrotron radiation-based micro computed tomography. Journal of Neuroscience Methods, 2008, 170, 149-155.	1.3	28
63	Damping of Selective-Laser-Melted NiTi for Medical Implants. Journal of Materials Engineering and Performance, 2014, 23, 2614-2619.	1.2	27
64	Binding and ordering of large organic molecules on an anisotropic metal surface: PVBA on Pd(110). Surface Science, 1999, 431, 168-173.	0.8	26
65	Comparing the accuracy of master models based on digital intra-oral scanners with conventional plaster casts. Physics in Medicine, 2016, 1, 20-26.	0.6	26
66	Tomography studies of human foreskin fibroblasts on polymer yarns. Nuclear Instruments & Methods in Physics Research B, 2003, 200, 397-405.	0.6	24
67	Three-Dimensional Characterization of Cell Clusters Using Synchrotron-Radiation-Based Micro-Computed Tomography. Microscopy and Microanalysis, 2006, 12, 97-105.	0.2	24
68	Combining micro computed tomography and three-dimensional registration to evaluate local strains in shape memory scaffolds. Acta Biomaterialia, 2014, 10, 1024-1034.	4.1	24
69	Tilting the jaw to improve the image quality or to reduce the dose in cone-beam computed tomography. European Journal of Radiology, 2011, 80, e389-e393.	1.2	23
70	The stiffness of bone marrow cell–knit composites is increased during mechanical load. Biomaterials, 2001, 22, 3169-3178.	5.7	22
71	Blood vessel staining in the myocardium for 3D visualization down to the smallest capillaries. Nuclear Instruments & Methods in Physics Research B, 2006, 246, 254-261.	0.6	22
72	The petrosal bone and bony labyrinth of early to middle Miocene European deer (Mammalia, Cervidae) reveal their phylogeny. Journal of Morphology, 2016, 277, 1329-1338.	0.6	22

#	Article	IF	CITATIONS
73	Epitaxial growth of para-hexaphenyl on GaAs(001)-2×4. Surface Science, 1999, 437, 191-197.	0.8	21
74	SPAâ€RHEED—A novel method in reflection highâ€energy electron diffraction with extremely high angular and energy resolution. Review of Scientific Instruments, 1995, 66, 5232-5235.	0.6	20
75	Strain relief in metal heteroepitaxy on faceâ€centeredâ€cubic(100): Cu/Ni(100). Journal of Vacuum Science and Technology A: Vacuum, Surfaces and Films, 1996, 14, 1878-1881.	0.9	20
76	Amino acid neurotransmitter metabolism in neurones and glia following kainate injection in rats. Neuroscience Letters, 2000, 279, 169-172.	1.0	20
77	Wood-Derived Porous Ceramics via Infiltration of SiO2-Sol and Carbothermal Reduction. Holzforschung, 2003, 57, 440-446.	0.9	20
78	Nanomethods: Scanning X-ray scattering: Evaluating the nanostructure of human tissues. European Journal of Nanomedicine, 2010, 3, .	0.6	20
79	Virtual histology of an entire mouse brain from formalin fixation to paraffin embedding. Part 1: Data acquisition, anatomical feature segmentation, tracking global volume and density changes. Journal of Neuroscience Methods, 2021, 364, 109354.	1.3	20
80	Optimization of the artificial urinary sphincter: modelling and experimental validation. Physics in Medicine and Biology, 2006, 51, 1361-1375.	1.6	19
81	Mineralization of Early Stage Carious Lesions In Vitro—A Quantitative Approach. Dentistry Journal, 2015, 3, 111-122.	0.9	19
82	Strain Relief via Island Ramification in Submonolayer Hereroepitaxy. Surface Review and Letters, 1998, 05, 769-781.	0.5	18
83	Surprising lack of liposome-induced complement activation by artificial 1,3-diamidophospholipids in vitro. Nanomedicine: Nanotechnology, Biology, and Medicine, 2016, 12, 845-849.	1.7	18
84	Impact of adhesive surface and volume of luting resin on fracture resistance of root filled teeth. International Endodontic Journal, 2011, 44, 432-439.	2.3	16
85	Gold Layers on Elastomers near the Critical Stress Regime. Advanced Materials Technologies, 2017, 2, 1700105.	3.0	16
86	Tailoring biocompatibility: Benefitting patients. Materials Today, 2010, 13, 58.	8.3	15
87	Immunological response to nitroglycerin-loaded shear-responsive liposomes in vitro and in vivo. Journal of Controlled Release, 2017, 264, 14-23.	4.8	15
88	Scavenging of Dickkopf-1 by macromer-based biomaterials covalently decorated with sulfated hyaluronan displays pro-osteogenic effects. Acta Biomaterialia, 2020, 114, 76-89.	4.1	15
89	A UHV STM for in situ characterization of MBE/CVD growth on 4-inch wafers. Applied Physics A: Materials Science and Processing, 1998, 66, S993-S997.	1.1	14

90 Contractile cell forces exerted on rigid substrates. , 2011, 21, 479-487.

14

#	Article	IF	CITATIONS
91	A comparative STM and SPA-LEED study on the evolution of strain induced stripe pattern on Cu/Ni(100). Surface Science, 1997, 376, 113-122.	0.8	13
92	High-sensitivity phase-contrast tomography of rat brain in phosphate buffered saline. Journal of Physics: Conference Series, 2009, 186, 012046.	0.3	13
93	Cracks in dentin and enamel after cryopreservation. Oral Surgery, Oral Medicine, Oral Pathology and Oral Radiology, 2012, 113, e5-e10.	0.2	13
94	Implementation of a double-grating interferometer for phase-contrast computed tomography in a conventional system nanotom® m. APL Bioengineering, 2018, 2, 016106.	3.3	13
95	Molecular beam epitaxy ofp-hexaphenyl on GaAs(111). Surface and Interface Analysis, 2000, 30, 518-521.	0.8	12
96	Micro- and nanostructured polymer substrates for biomedical applications. Proceedings of SPIE, 2012,	0.8	12
97	Assessing the morphology of selective laser melted NiTi-scaffolds for a three-dimensional quantification of the one-way shape memory effect. , 2013, , .		12
98	Molecular beam deposition of high-permittivity polydimethylsiloxane for nanometer-thin elastomer films in dielectric actuators. Materials and Design, 2016, 105, 106-113.	3.3	12
99	Single and double grating-based X-ray microtomography using synchrotron radiation. Applied Physics Letters, 2017, 110, .	1.5	12
100	Sensitivity comparison of absorption and grating-based phase tomography of paraffin-embedded human brain tissue. Applied Physics Letters, 2019, 114, .	1.5	12
101	Trench formation in surfactant mediated epitaxial film growth of Ge on Si(100). Applied Physics A: Solids and Surfaces, 1992, 54, 265-269.	1.4	11
102	Comparison of reflection high-energy electron diffraction and low-energy electron diffraction using high-resolution instrumentation. Surface Science, 1997, 389, 338-348.	0.8	11
103	Determination of strain fields in porous shape memory alloys using micro-computed tomography. Proceedings of SPIE, 2010, , .	0.8	11
104	Nanostructuring polyetheretherketone for medical implants. European Journal of Nanomedicine, 2012, 4, .	0.6	11
105	Midâ€regional proâ€atrial natriuretic peptide and the assessment of volaemic status and differential diagnosis of profound hyponatraemia. Journal of Internal Medicine, 2015, 278, 29-37.	2.7	11
106	Three-dimensional imaging and analysis of entire peripheral nerves after repair and reconstruction. Journal of Neuroscience Methods, 2018, 295, 37-44.	1.3	11
107	Shedding Light on Metalâ€Based Nanoparticles in Zebrafish by Computed Tomography with Micrometer Resolution. Small, 2020, 16, e2000746.	5.2	11
108	Virtual histology of an entire mouse brain from formalin fixation to paraffin embedding. Part 2: Volumetric strain fields and local contrast changes. Journal of Neuroscience Methods, 2022, 365, 109385.	1.3	11

#	Article	IF	CITATIONS
109	In-plane alignment of noncentrosymmetric molecules by oblique-incidence molecular beam deposition. Applied Physics Letters, 1999, 74, 3110-3112.	1.5	10
110	Tomography studies of biological cells on polymer scaffolds. Journal of Physics Condensed Matter, 2004, 16, S3499-S3510.	0.7	10
111	Comparative micro computed tomography study of a vertebral body. Proceedings of SPIE, 2008, , .	0.8	10
112	Bio-inspired dental fillings. Proceedings of SPIE, 2009, , .	0.8	10
113	Systemic allergic dermatitis reaction to nickel released from an eyelet in an intravenous catheter. Contact Dermatitis, 2009, 61, 180-182.	0.8	10
114	Evaluating the microstructure of human brain tissues using synchrotron radiation-based micro-computed tomography. Proceedings of SPIE, 2010, , .	0.8	10
115	Morphology of urethral tissues. Proceedings of SPIE, 2010, , .	0.8	10
116	Thin Film Formation and Morphology of Electrosprayed Polydimethylsiloxane. Langmuir, 2016, 32, 3276-3283.	1.6	10
117	Three-dimensional and non-destructive characterization of nerves inside conduits using laboratory-based micro computed tomography. Journal of Neuroscience Methods, 2018, 294, 59-66.	1.3	10
118	Spatially resolved small-angle X-ray scattering for characterizing mechanoresponsive liposomes using microfluidics. Materials Today Bio, 2019, 1, 100003.	2.6	10
119	Optimizing contrast and spatial resolution in hard x-ray tomography of medically relevant tissues. Applied Physics Letters, 2020, 116, .	1.5	10
120	Histology to μCT Data Matching Using Landmarks and a Density Biased RANSAC. Lecture Notes in Computer Science, 2014, 17, 243-250.	1.0	10
121	Visualising complex morphology of fatigue cracks in voxel based 3D datasets. Materials Science and Technology, 2006, 22, 1038-1044.	0.8	9
122	Disposable polymeric micro-cantilever arrays for sensing. Procedia Engineering, 2010, 5, 347-350.	1.2	9
123	Morphology and conductivity of Au films on polydimethylsiloxane using (3-mercaptopropyl)trimethoxysilane (MPTMS) as an adhesion promoter. Proceedings of SPIE, 2016, , .	0.8	9
124	Crosslinkable polymeric contrast agent for high-resolution X-ray imaging of the vascular system. Chemical Communications, 2020, 56, 5885-5888.	2.2	9
125	Ge-Quantum Dots on SI(001) Tailored by Carbon Predeposition. Materials Research Society Symposia Proceedings, 1998, 533, 183.	0.1	8
126	Degradation Kinetics of Biodegradable Fiber Composites. Journal of Polymers and the Environment, 2000, 8, 91-96.	2.4	8

#	Article	IF	CITATIONS
127	Designing micro- and nanostructures for artificial urinary sphincters. Proceedings of SPIE, 2012, , .	0.8	8
128	Stress measurements of planar dielectric elastomer actuators. Review of Scientific Instruments, 2016, 87, 053901.	0.6	8
129	Tailoring the mass distribution and functional group density of dimethylsiloxane-based films by thermal evaporation. APL Materials, 2016, 4, .	2.2	8
130	Automatic deformable registration of histological slides to μCT volume data. Journal of Microscopy, 2018, 271, 49-61.	0.8	8
131	Strain-induced dimer adatom stacking fault structures of germanium on Si(111)-(â^š3×â^š3)R30°:B observed by scanning tunneling microscopy. Journal of Vacuum Science & Technology an Official Journal of the American Vacuum Society B, Microelectronics Processing and Phenomena, 1992, 10, 16.	1.6	7
132	Film thickness measurement and linear dichroism of organic thin films prepared by molecular beam deposition at oblique incidence. Optical Materials, 1999, 12, 345-350.	1.7	7
133	The cochlea in fetuses with neural tube defects. International Journal of Developmental Neuroscience, 2009, 27, 669-676.	0.7	7
134	Pelizaeus Merzbacher disease: morphological analysis of the vestibulo-cochlear system. Acta Oto-Laryngologica, 2009, 129, 1395-1399.	0.3	7
135	Realâ€time measurements of human chondrocyte heat production during in vitro proliferation. Biotechnology and Bioengineering, 2011, 108, 3019-3024.	1.7	7
136	Nano-Mechanical Transduction of Polymer Micro-Cantilevers to Detect Bio-Molecular Interactions. Biointerphases, 2012, 7, 6.	0.6	7
137	Mechanical and chemical stability of injectionâ€molded microcantilevers used for sensing. Journal of Applied Polymer Science, 2013, 127, 2363-2370.	1.3	7
138	Nanomechanical probing of thin-film dielectric elastomer transducers. Applied Physics Letters, 2017, 111, .	1.5	7
139	A quantitative correction for phase wrapping artifacts in hard X-ray grating interferometry. Applied Physics Letters, 2018, 113, .	1.5	7
140	Allometric and Phylogenetic Aspects of Stapes Morphology in Ruminantia (Mammalia, Artiodactyla). Frontiers in Earth Science, 2020, 8, .	0.8	7
141	Simultaneous Three-Dimensional Vascular and Tubular Imaging of Whole Mouse Kidneys With X-ray μCT. Microscopy and Microanalysis, 2020, 26, 731-740.	0.2	7
142	Observations on the scaling relationship between bony labyrinth, skull size and body mass in ruminants. , 2019, , .		7
143	Comparative hard x-ray tomography for virtual histology of zebrafish larva, human tooth cementum, and porcine nerve. Journal of Medical Imaging, 2022, 9, 031507.	0.8	7
144	Anatomy of the murine and human cochlea visualized at the cellular level by synchrotron-radiation-based micro-computed tomography. , 2006, , .		6

#	Article	IF	CITATIONS
145	Bio-mimetic hollow scaffolds for long bone replacement. Proceedings of SPIE, 2009, , .	0.8	6
146	X-ray grating interferometer for imaging at a second-generation synchrotron radiation source. Proceedings of SPIE, 2010, , .	0.8	6
147	Morphology of atherosclerotic coronary arteries. Proceedings of SPIE, 2012, , .	0.8	6
148	Comparison of denture models by means of micro computed tomography. , 2012, , .		6
149	Tailoring surface nanostructures on polyaryletherketones for load-bearing implants. European Journal of Nanomedicine, 2014, 6, .	0.6	6
150	Timeâ€Resolved Plasmonics used to Onâ€Line Monitor Metal/Elastomer Deposition for Lowâ€Voltage Dielectric Elastomer Transducers. Advanced Electronic Materials, 2017, 3, 1700073.	2.6	6
151	Automated Analysis of Spatially Resolved X-ray Scattering and Micro Computed Tomography of Artificial and Natural Enamel Carious Lesions. Journal of Imaging, 2018, 4, 81.	1.7	6
152	Small-Angle Neutron Scattering Study of Temperature-Induced Structural Changes in Liposomes. Langmuir, 2019, 35, 11210-11216.	1.6	6
153	Ex vivo evaluation of an atherosclerotic human coronary artery via histology and high-resolution hard X-ray tomography. Scientific Reports, 2019, 9, 14348.	1.6	6
154	Toward genome editing in X-linked RP—development of a mouse model with specific treatment relevant features. Translational Research, 2019, 203, 57-72.	2.2	6
155	Hierarchically structured polydimethylsiloxane films for ultra-soft neural interfaces. Micro and Nano Engineering, 2020, 7, 100051.	1.4	6
156	Accuracy of commercial intraoral scanners. Journal of Medical Imaging, 2021, 8, 035501.	0.8	6
157	Three-dimensional morphology and mechanics of bone scaffolds fabricated by rapid prototyping. International Journal of Materials Research, 2012, 103, 200-206.	0.1	6
158	NUCLEATION AND GROWTH OF Cu/Ni(100): A VARIABLE TEMPERATURE STM STUDY. Surface Review and Letters, 1997, 04, 1161-1165.	0.5	5
159	Ordering of PVBA on amorphous SiO2 and Pd(110). Thin Solid Films, 1999, 343-344, 171-174.	0.8	5
160	Three-dimensional assessment of brain tissue morphology. , 2006, 6318, 9.		5
161	Minipig urethra: A suitable animal model in vitro. Technology and Health Care, 2007, 20, 329-336.	0.5	5
162	Grating-based tomography of human tissues. AIP Conference Proceedings, 2012, , .	0.3	5

#	Article	IF	CITATIONS
163	Micro- and nanostructured electro-active polymer actuators as smart muscles for incontinence treatment. AIP Conference Proceedings, 2015, , .	0.3	5
164	Multimodal imaging of the human knee down to the cellular level. Journal of Physics: Conference Series, 2017, 849, 012026.	0.3	5
165	Hard X-ray Nano-Holotomography of Formalin-Fixated and Paraffin-Embedded Human Brain Tissue. Microscopy and Microanalysis, 2018, 24, 354-355.	0.2	5
166	PDE10A mutation in two sisters with a hyperkinetic movement disorder - Response to levodopa. Parkinsonism and Related Disorders, 2019, 63, 240-242.	1.1	5
167	Mechanistic Illustration: How Newly-Formed Blood Vessels Stopped by the Mineral Blocks of Bone Substitutes Can Be Avoided by Using Innovative Combined Therapeutics. Biomedicines, 2021, 9, 952.	1.4	5
168	Conducting and stretchable nanometer-thin gold/thiol-functionalized polydimethylsiloxane films. Journal of Nanophotonics, 2018, 12, 1.	0.4	5
169	Three-dimensional analysis of aligner gaps and thickness distributions, using hard x-ray tomography with micrometer resolution. Journal of Medical Imaging, 2022, 9, .	0.8	5
170	Functional micro-imaging of soft and hard tissue using synchrotron light. , 2004, , .		4
171	3D analysis of bone formation around titanium implants using micro computed tomography (μCT). , 2006, , .		4
172	Quality assessment of clinical computed tomography. Proceedings of SPIE, 2008, , .	0.8	4
173	Comparative study of desktop- and synchrotron radiation-based micro computed tomography analyzing cell-seeded scaffolds in tissue engineering of bone. , 2008, , .		4
174	Evaluating tooth restorations: micro-computed tomography in practical training for students in dentistry. , 2010, , .		4
175	Nanodentistry. Nanoscience and Technology, 2012, , 95-107.	1.5	4
176	Comparison of propagation-based phase-contrast tomography approaches for the evaluation of dentin microstructure. Proceedings of SPIE, 2012, , .	0.8	4
177	Comparing the micro-vascular structure of cancerous and healthy tissues. Proceedings of SPIE, 2012, , \cdot	0.8	4
178	Asymmetric rotational axis reconstruction of grating-based x-ray phase contrast tomography of the human cerebellum. Proceedings of SPIE, 2012, , .	0.8	4
179	Combined micro computed tomography and histology study of bone augmentation and distraction osteogenesis. , 2012, , .		4
180	Global and local hard X-ray tomography of a centimeter-size tumor vessel tree. Journal of Synchrotron Radiation, 2012, 19, 114-125.	1.0	4

#	Article	IF	CITATIONS
181	Leakage current, self-clearing and actuation efficiency of nanometer-thin, low-voltage dielectric elastomer transducers tailored by thermal evaporation. Proceedings of SPIE, 2017, , .	0.8	4
182	Biomimetic nanostructures for the silicone-biosystem interface: tuning oxygen-plasma treatments of polydimethylsiloxane. European Journal of Nanomedicine, 2017, 9, .	0.6	4
183	Polydimethylsiloxane films engineered for smart nanostructures. Microelectronic Engineering, 2018, 194, 1-7.	1.1	4
184	Immunocompatibility of Rad-PC-Rad liposomes in vitro, based on human complement activation and cytokine release. Precision Nanomedicine, 2018, 1, 43-62.	0.4	4
185	Imaging the internal structure of Borelis schlumbergeri Reichel (1937): Advances by high-resolution hard X-ray microtomography. Palaeontologia Electronica, 2019, 22, .	0.9	4
186	Inelastic Scattering in Reflection High-Energy Electron Diffraction from Si(111). Physical Review Letters, 1997, 79, 4393-4396.	2.9	3
187	Internal structures of scaffold-free 3D cell cultures visualized by synchrotron radiation-based micro-computed tomography. , 2008, , .		3
188	Synchrotron radiation-based micro computed tomography in the assessment of dentin de- and re-mineralization. , 2008, , .		3
189	The morphology of amputated human teeth and its relation to mechanical properties after restoration treatment. , 2010, , .		3
190	Computed tomography to quantify tooth abrasion. Proceedings of SPIE, 2010, , .	0.8	3
191	Grating interferometry-based phase microtomography of atherosclerotic human arteries. Proceedings of SPIE, 2014, , .	0.8	3
192	Ultraviolet–ozone surface cleaning of injectionâ€molded, thermoplastic microcantilevers. Journal of Applied Polymer Science, 2015, 132, .	1.3	3
193	Hierarchical imaging of the human knee. , 2016, , .		3
194	X-ray micro-tomography for investigations of brain tissues on cellular level. , 2016, , .		3
195	Biomimetic artificial sphincter muscles: status and challenges. Proceedings of SPIE, 2016, , .	0.8	3
196	Extended-field synchrotron microtomography for non-destructive analysis of incremental lines in archeological human teeth cementum. , 2021, , .		3
197	Impact of fixation and paraffin embedding on mouse brain morphology: a synchrotron radiation-based tomography study. , 2021, , .		3
198	Image Based Analysis of Bone Graft Samples made by 3D Printing Using Conventional and Synchrotron-Radiation-Based Micro-Computed Tomography. , 2007, , 121-126.		3

#	Article	IF	CITATIONS
199	Imaging the Human Body: Micro- and Nanostructure of Human Tissues. Nanoscience and Technology, 2012, , 69-94.	1.5	3
200	Recent trends in high-resolution hard x-ray tomography. , 2019, , .		3
201	Comparing the accuracy of intraoral scanners, using advanced micro computed tomography. , 2019, , .		3
202	On the thermal behaviour of molecular beam effusion sources. Crystal Research and Technology, 1990, 25, 1087-1095.	0.6	2
203	Image-based analysis of the internal microstructure of bone replacement scaffolds fabricated by 3D printing. , 2006, 6318, 64.		2
204	Angiofil: a novel radio-contrast agent for post-mortem micro-angiography. Proceedings of SPIE, 2008, ,	0.8	2
205	Simulation of stress urinary incontinence for in-vitro studies. Technology and Health Care, 2008, 16, 77-83.	0.5	2
206	Evaluation of oral scanning in comparison to impression using three-dimensional registration. Proceedings of SPIE, 2012, , .	0.8	2
207	High-resolution x-ray computed tomography to understand ruminant phylogeny. Proceedings of SPIE, 2014, , .	0.8	2
208	Characterization of a human tooth with carious lesions using conventional and synchrotron radiation-based micro computed tomography. Proceedings of SPIE, 2014, , .	0.8	2
209	Assessing the grain structure of highly X-ray absorbing metallic alloys. International Journal of Materials Research, 2014, 105, 692-701.	0.1	2
210	Impact of electrode preparation on the bending of asymmetric planar electro-active polymer microstructures. Proceedings of SPIE, 2014, , .	0.8	2
211	Comparing natural and artificial carious lesions in human crowns by means of conventional hard x-ray micro-tomography and two-dimensional x-ray scattering with synchrotron radiation. , 2016, , .		2
212	Middle ear bones of a mid-gestation ruminant foetus extracted from x-ray computed tomography. , 2016, , .		2
213	Characterization of mechano-sensitive nano-containers for targeted vasodilation. Proceedings of SPIE, 2016, , .	0.8	2
214	Non-destructive phase contrast hard x-ray imaging to reveal the three-dimensional microstructure of soft and hard tissues. , 2016, , .		2
215	Liposomes: bio-inspired nano-containers for physically triggered targeted drug delivery. , 2017, , .		2
216	Electrospraying and ultraviolet light curing of nanometer-thin polydimethylsiloxane membranes for low-voltage dielectric elastomer transducers. , 2017, , .		2

#	Article	IF	CITATIONS
217	Submonolayer Nucleation and Growth of Copper on Ni(100). NATO ASI Series Series B: Physics, 1997, , 151-159.	0.2	2
218	Evaluation of metal nanoparticle- and plastic resin-based x-ray contrast agents for kidney capillary imaging. , 2019, , .		2
219	Imaging the orientation of myelin sheaths in a non-stained histology slide of human brain. Precision Nanomedicine, 0, , .	0.4	2
220	Combining High-Resolution Hard X-ray Tomography and Histology for Stem Cell-Mediated Distraction Osteogenesis. Applied Sciences (Switzerland), 2022, 12, 6286.	1.3	2
221	Visualization of tumor vessels using synchrotron radiation-based micro computed tomography. Journal of Physics: Conference Series, 2009, 186, 012088.	0.3	1
222	The microstructure of mandibular bone grafts and three-dimensional cell clusters. , 2010, , .		1
223	Mikro-Computertomographie für die dreidimensionale Charakterisierung von Implantaten und Geweben. Sports Orthopaedics and Traumatology, 2010, 26, 145-151.	0.1	1
224	X-ray Grating Interferometry at ESRF: Applications and Recent Technical Developments. , 2011, , .		1
225	Anisotropy in polyetheretherketone films. Journal of Nanophotonics, 2012, 6, 063510.	0.4	1
226	Nanometer-size anisotropy of injection-molded polymer micro-cantilever arrays. Journal of Applied Physics, 2012, 111, 103530.	1.1	1
227	Shear Stress as Drug Delivery Trigger. Chimia, 2012, 66, 715.	0.3	1
228	Controlling Mechanical Properties of NiTi Scaffolds built by Selective Laser Melting. Biomedizinische Technik, 2012, 57, .	0.9	1
229	Measuring the bending of asymmetric planar EAP structures. Proceedings of SPIE, 2013, , .	0.8	1
230	Three-dimensional imaging of human hippocampal tissue using synchrotron radiation- and grating-based micro computed tomography. Proceedings of SPIE, 2014, , .	0.8	1
231	Three-dimensional registration of synchrotron radiation-based micro-computed tomography images with advanced laboratory micro-computed tomography data from murine kidney casts. , 2014, , .		1
232	Strain-dependent characterization of electrode and polymer network of electrically activated polymer actuators. Proceedings of SPIE, 2015, , .	0.8	1
233	X-ray microscopy of soft and hard human tissues. AIP Conference Proceedings, 2016, , .	0.3	1
234	Hard x-ray micro-tomography of a human head post-mortem as a gold standard to compare x-ray		1

modalities. , 2016, , .

#	Article	IF	CITATIONS
235	Automatic histology registration in application to x-ray modalities. Proceedings of SPIE, 2016, , .	0.8	1
236	Characterization of ultraviolet light cured polydimethylsiloxane films for low-voltage, dielectric elastomer actuators. , 2016, , .		1
237	Hard X-ray submicrometer tomography of human brain tissue at Diamond Light Source. Journal of Physics: Conference Series, 2017, 849, 012030.	0.3	1
238	Visualization and Segmentation of Cells in Unstained Paraffin-Embedded Cerebral Tissue. Microscopy and Microanalysis, 2018, 24, 408-409.	0.2	1
239	Hard X-ray microtomography of Zebrafish larvae. , 2021, , .		1
240	Grating-based tomography applications in biomedical engineering. , 2017, , .		1
241	Phase-contrast x-ray tomography reveals the micro-anatomy of soft tissues. SPIE Newsroom, 0, , .	0.1	1
242	Recent trends in high-resolution x-ray tomography. , 2017, , .		1
243	Innervation of the $cow \hat{a} \in \mathbb{T}$ s inner ear derived from micro-computed tomography. , 2017, , .		1
244	Three-dimensional characterization of soft silicone elements for intraoral device. , 2019, , .		1
245	Bone marrow derived mesenchymal stem cells isolated from patients with diabetes mellitus type 1 are able to induce a pancreatic endocrine genes in vitro. Journal of Stem Cells and Regenerative Medicine, 2007, 2, 102-3.	2.2	1
246	In Vivo Toxicity of Titanium Dioxide and Gold Nanoparticles. , 2012, , 1083-1090.		0
247	Insect Flight and Micro Air Vehicles (MAVs). , 2012, , 1096-1109.		Ο
248	Equipment automation framework with embedded Interface-A. , 2013, , .		0
249	Tumors in murine brains studied by grating-based phase contrast microtomography. , 2014, , .		0
250	Computational cell quantification in the human brain tissues based on hard x-ray phase-contrast tomograms. Proceedings of SPIE, 2016, , .	0.8	0
251	Electro-spraying and ultra-violet light curing of polydimethylsiloxane to fabricate thin films for low-voltage dielectric elastomer actuators. , 2016, , .		Ο
252	Histology-validated x-ray tomography for imaging human coronary arteries. Proceedings of SPIE, 2016, , .	0.8	0

#	Article	IF	CITATIONS
253	Imaging tissues for biomedical research using the high-resolution micro-tomography system nanotom \hat{A}^{\circledast} m. Proceedings of SPIE, 2016, , .	0.8	о
254	Nanostructure Formation: Timeâ€Resolved Plasmonics used to Onâ€Line Monitor Metal/Elastomer Deposition for Lowâ€Voltage Dielectric Elastomer Transducers (Adv. Electron. Mater. 8/2017). Advanced Electronic Materials, 2017, 3, .	2.6	0
255	X-ray micro computed tomography for the visualization of an atherosclerotic human coronary artery. Journal of Physics: Conference Series, 2017, 849, 012002.	0.3	Ο
256	Propagation-based X-ray Phase Contrast Microtomography of Zebrafish Embryos to Understand Drug Delivery. Microscopy and Microanalysis, 2018, 24, 406-407.	0.2	0
257	Double Grating Interferometry in a Commercial Micro Computed Tomography System for Biomedical Imaging. Microscopy and Microanalysis, 2018, 24, 388-389.	0.2	0
258	1. Nanomedicine at a glance. , 2018, , 3-15.		0
259	Volumetric Nanoscale Imaging: Hard X-Ray Nanoholotomography: Large-Scale, Label-Free, 3D Neuroimaging beyond Optical Limit (Adv. Sci. 6/2018). Advanced Science, 2018, 5, 1870036.	5.6	0
260	Historic beaten-copper cranium. , 2021, , .		0
261	Imaging the Human Body Down to the Molecular Level. , 2016, , 1-10.		0
262	Imaging the Human Body Down to the Molecular Level. , 2016, , 1501-1510.		0
263	High-resolution synchrotron radiation-based phase tomography of the healthy and epileptic brain. , 2016, , .		0
264	Removing ring artefacts from synchrotron radiation-based hard x-ray tomography data. , 2017, , .		0
265	Imaging cellular and subcellular structure of human brain tissue using micro computed tomography. , 2017, , .		Ο
266	Highly compliant nanometer-thin Au electrodes exploiting the binding to thiol-functionalized polydimethylsiloxane films. , 2018, , .		0
267	Special Section Guest Editorial: Nanoscience and Biomaterials in Photonics. Journal of Nanophotonics, 2018, 12, 1.	0.4	Ο
268	Zugangsrealitäzu S3 Leitlinien gerechten Adipositasoperationen in Deutschland. Zeitschrift Fur Gastroenterologie, 2019, 57, .	0.2	0
269	Correction of phase wrapping artifacts in grating-based hard x-ray tomography. , 2019, , .		Ο
270	Cone-beam computed tomography - magnetic resonance imaging registration in dento-maxillary imaging. , 2019, , .		0

#	Article	IF	CITATIONS
271	Reentry of endodontic access cavities: composite residue and loss of tooth substance. Swiss Dental Journal, 2021, 131, .	0.4	0
272	Three-dimensional imaging and analysis of annual layers in tree trunk and tooth cementum. , 2022, , .		0